REPORT DOCUMENTATION PAGE

1. REPORT DATE (DD-MM-YYYY)	2. REPORT TYPE	3. DATES COVERED (From - To)
Aug 2009	REPRINT	

4. TITLE AND SUBTITLE
Mass Spectrometric Analysis of the Electrospray Plume from an Externally Wetted Tungsten Ribbon Emitter

5a. CONTRACT NUMBER

5b. GRANT NUMBER

5c. PROGRAM ELEMENT NUMBER
61102F

6. AUTHORS
Brian W. Ticknor
Shawn W. Miller
Yu-Hui Chiu

5d. PROJECT NUMBER
2303

5e. TASK NUMBER
RS

5f. WORK UNIT NUMBER
A1

7. PERFORMING ORGANIZATION NAME(S) AND ADDRESS(ES)

Air Force Research Laboratory /RVBXT
29 Randolph Road
Hanscom AFB, MA 01731-3010

8. PERFORMING ORGANIZATION REPORT NUMBER
AFRL-RV-HA-TR-2009-1118

9. SPONSORING/MONITORING AGENCY NAME(S) AND ADDRESS(ES)

10. SPONSOR/MONITOR'S ACRONYM(S)
AFRL/RVBXT

11. SPONSOR/MONITOR'S REPORT NUMBER(S)

12. DISTRIBUTION/AVAILABILITY STATEMENT
Approved for Public Release; distribution unlimited.

20091207057

13. SUPPLEMENTARY NOTES
Presented at 46th AIAA/ASME/ASEE Joint Propulsion Conference and Exhibit, Denver, CO, Aug 2009.

14. ABSTRACT Angle-resolved mass spectrometry in conjunction with retarding potential energy analysis provides information on the mechanisms of ion field evaporation and spatial distributions of the emitted ions and droplets, the latter being of particular importance in the emitter array configuration. In the present study, we conduct mass spectrometric, retarding potential, and angular distribution measurements for ions emitted from [Emim][Im] (1-ethyl-3-methylimidazolium bis(trifluromethylsufonyl)imide) when sprayed from an externally wetted tungsten ribbon emitter. A tungsten ribbon of 750 μm width and 50 μm thickness is electrochemically etched to produce the ribbon emitter tip $\sim$20 μm wide and $\sim$1 μm thick. The angle resolved measurements indicate that the spray comprises a mixture of droplets and ions. The major ionic species identified are $Emim^+$ $([Emim][Im])_n$ and $Im^-([Emim][Im])_n$ with n=0,1,2 in the positive and negative polarity modes, respectively. At low extraction voltage (1070-1170 V), the dominate ion intensity comprises a narrow distribution in the center of the spray, with additional intensity emitted at larger angles ($>\pm$10 degrees). The anionic species observed are Im^- and $Im^-([Emim][Im])$ with approximately equal intensity. At higher extraction energies ($\sim$1300-1400 V), a broader angular distribution is found, extending to 40 degree half-angles. The distribution is peaked at center of the spray. In this case, $Im^-([Emim][Im])$ and $Im^-([Emim][Im])_2$ are the major species observed. The total current and deposition measurements are consistent with the observation that the higher extraction voltage creates a larger flow rate than that produced from the lower extraction voltage, leading to emission that contains a larger fraction of droplets versus ions, and also produces droplets of a larger size.

15. SUBJECT TERMS

Mass spectrometry   Electrospray plume   Externally wetted tungsten ribbon emitter
1-ethyl-3-methylimidazolium bis(trifluromethylsulfonyl)imide)

16. SECURITY CLASSIFICATION OF:			17. LIMITATION OF ABSTRACT	18. NUMBER OF PAGES	19a. NAME OF RESPONSIBLE PERSON
a. REPORT	b. ABSTRACT	c. THIS PAGE			Yu-hui Chiu
UNCL	UNCL	UNCL	UNL		19B. TELEPHONE NUMBER (Include area code)

Standard Form 298 (Rev. 8/98)
Prescribed by ANSI Std. Z39.18

DTIC COPY

Mass Spectrometric Analysis of the Electrospray Plume from an Externally Wetted Tungsten Ribbon Emitter

Brian W. Ticknor[1], Shawn W. Miller[2], and Yu-Hui Chiu[3]

Air Force Research Laboratory, Space Vehicles Directorate, Hanscom AFB, Massachusetts, 01731

Angle-resolved mass spectrometry in conjunction with retarding potential energy analysis provides information on the mechanisms of ion field evaporation and spatial distributions of the emitted ions and droplets, the latter being of particular importance in the emitter array configuration. In the present study, we conduct mass spectrometric, retarding potential, and angular distribution measurements for ions emitted from [Emim][Im] (1-ethyl-3-methylimidazolium bis(trifluromethylsulfonyl)imide) when sprayed from an externally wetted tungsten ribbon emitter. A tungsten ribbon of 750 μm width and 50 μm thickness is electrochemically etched to produce the ribbon emitter tip ~20 μm wide and ~1 μm thick. The angle resolved measurements indicate that the spray comprises a mixture of droplets and ions. The major ionic species identified are $Emim^+([Emim][Im])_n$ and $Im^-([Emim][Im])_n$, with n=0,1,2 in the positive and negative polarity modes, respectively. At low extraction voltage (1070-1170 V), the dominate ion intensity comprises a narrow distribution in the center of the spray, with additional intensity emitted at larger angles (>±10 degrees). The anionic species observed are Im^- and $Im^-([Emim][Im])$ with approximately equal intensity. At higher extraction voltages (~1300-1400 V), a broader angular distribution is found, extending to 40 degree half-angles. The distribution is peaked at center of the spray. In this case, $Im^-([Emim][Im])$ and $Im^-([Emim][Im])_2$ are the major species observed. The total current and deposition measurements are consistent with the observation that the higher extraction voltage creates a larger flow rate than that produced from the lower extraction voltage, leading to emission that contains a larger fraction of droplets versus ions, and also produces droplets of a larger size.

Nomenclature

I_{sp}	=	specific impulse
m/q	=	mass to charge ratio
V_{ext}	=	total extraction voltage

I. Introduction

DUE to their unique physical properties such as low vapor pressure and high conductivities, ionic liquids (ILs) are a very attractive propellant for colloid thruster applications. In these systems, a high electric field is applied to the surface of an IL, inducing a Taylor cone[1] and resulting in emission of charged droplets and ions, which are then electrostatically accelerated to produce thrust. Because of the use of electrospray ionization technology,[2] colloid thrusters are also known as electrospray thrusters. The IL 1-ethyl-3methylimidazolium bis(trifluoromethylsulfonyl)imide ([Emim][Im]) has passed all space exposure tests and is the propellant choice for the upcoming Jet Propulsion Laboratory ST7 Disturbance Reduction Mission.[3, 4] IL electrospray thrusters can be operated in an ion-only mode (high I_{sp}), a mixed ion-droplet mode, and a pure droplet mode (high thrust).[3] It was demonstrated that these different emission modes can be achieved by controlling the physical properties of the IL propellants, such as liquid flow rate.[5] Different flow rates of the IL account for the different emission modes, with

[1] National Research Council Postdoctoral Associate, Space Vehicles Directorate, AFRL/RVBXT, 29 Randolph Road, Hanscom AFB, MA 01731, AIAA Member.

[2] Space Scholar, Space Vehicles Directorate, AIAA Member.

[3] Task Scientist, Space Vehicles Directorate, AIAA Member.

low flow rates necessary to achieve ion-only emission. The ability of a single fuel to operate under these various conditions can lead to great flexibility in the types of missions on which it can be employed. Since the initial proposal by Fernández de la Mora of using electrosprayed ILs as a propulsion method for spacecraft,[5] a number of groups have studied these systems.[3, 6-12] Both laboratory and theoretical investigations of electrosprayed ILs are essential for developing an understanding of the ionization processes involved, as well as the factors that govern the production of droplets versus ions. In the present work, the electrospray properties of [Emim][Im] emitted from an externally wetted, sharpened tungsten ribbon are studied.

The choice of IL, the emitter geometry and material, extraction voltages applied to the ion source, and the temperature of the IL can be important parameters which dramatically influence the emission characteristics of the system.[8-10, 12] Several different emitter constructs, including capillaries,[5, 6, 13] cylindrical needles,[3, 7-12, 14] and metallic ribbons[15, 16] have all been suggested as candidates for thruster tips. Capillary emitters, where the IL is flowed through a hollow capillary, have been successfully utilized in some applications, but are limited to a less viscous IL application and by the need for flow controls. Externally wetted tungsten needles have shown excellent emission stability in the laboratory, but the thrust per needle produced remains low, on the order of 0.1 μN.[16] An array of externally wetted emitters, which has been successfully constructed, is one solution to this problem.[15, 16] These arrays have typically used linear, or ribbon-like emitters, which can accommodate a higher liquid flow rate to the thruster tip. The higher flow rate has been shown to give much higher currents per emitter as compared to the needles.[15] The electrospray parameters of a single ribbon emitter are not well characterized, however. The angular distribution of the spray has implications for the packing geometry which will optimize thruster performance in a multi-emitter array. One drawback of the external wetting technique is the difficulty in controlling the flow of the IL from a reservoir to the thruster tip. Successful operation depends on capillary action to draw the liquid to the tip, which can be thought of as a balance between the surface tension of the IL and the applied electric field. Thus, it should be possible to exert some level of control over the liquid flow rate by changing the extraction voltage used for emission. If successful, it might be possible to use the voltage to drive the emission mode of the thruster between the various ion-only, mixed ion-droplet, and pure droplet regimes.

In this work, mass spectrometric, retarding potential, and angular distribution measurements are conducted for [Emim][Im] electrosprayed from a single wetted tungsten ribbon. Characterization of the differences in spray dynamics between a needle and a ribbon emitter is important for advancing the understanding of the electrohydrodynamic processes which govern the electrospray thruster operation. Additionally, the experimental evidence shows that adjusting the extraction voltage can change the liquid flow rate to the thruster tip, and can successfully shift the emission mode, allowing an additional measure of control, presently lacking, over the operation of an externally wetted ribbon emitter.

II. Experimental

The experimental apparatus has been described in detail previously.[3, 9, 10] Briefly, the electrospray thruster source utilizes an externally wetted tungsten ribbon, 750 μm wide and 50 μm thick, that is electrochemically etched to produce a sharp tip.[8] The tip is approximately 20 μm along the width of the ribbon and ~1 μm thick. A 10 mil diameter length of tungsten wire is spot welded approximately 3 mm from the tip of the emitter, with the wire junction serving as a support for a drop of the [Emim][Im] propellant. The tip is wetted by heating the ribbon and then placing a drop of liquid on the junction, taking care to spread it all the way to the end. Capillary action and the roughness of the etched metal surface aid the flow of the IL to the emitter tip. The thruster is aligned and positioned ~1 mm from the extractor electrode with a 2 mm diameter aperture. The entire source assembly, including the ribbon and the extractor electrode, is rotatable with respect to the center axis of the experimental apparatus. Angles of approximately ± 50 degrees are achieved, which allows for the measurement of the ion emission properties of the Taylor cone-jet as a function of emitter angle. To study any differences in the thruster spray arising from the ribbon orientation, it may be
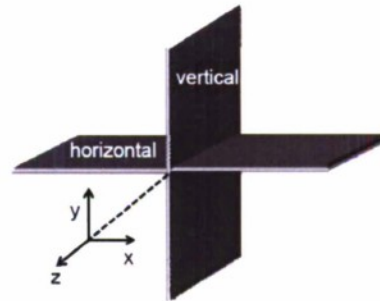

Figure 1. Schematic depiction of the two ribbon orientations used in the experiment. The center line of the experimental apparatus is the z axis, also the center (0 degree angle) of the thruster spray. The thruster rotation is always in the xz plane. The horizontal orientation has the width of the ribbon in the xz plane, parallel with the plane of rotation. The vertical orientation has the width of the ribbon in the yz plane, perpendicular to the plane of rotation.

mounted vertically, with the width of the ribbon edge perpendicular to the plane of the source rotation, or horizontally, where the width of the ribbon edge is parallel to the plane of the source rotation. The two orientations are depicted schematically in Fig. 1. The entire ion extraction source is held in vacuum of ~1 x 10^{-7} Torr.

Extraction voltages of ± 1070 – 1400 V are used, operated in constant polarity (DC) mode. The tungsten tip is biased at ± 500 volts, with the extractor biased at 570 – 900 V of the opposite polarity. The ± 500 V needle potential is chosen to maximize both mass resolution and ion signal through the mass spectrometer. The total emission current is determined from an electrometer measurement in the emitter power supply biasing circuit, and represents the total amount of current emitted by the thruster, integrated over all angles. Typical total emission currents observed from the ribbon emitter are ~150 – 350 nAmps, depending on the exact V_{ext} chosen. Previous work on needle emitters utilizing [Emim][Im] has shown that long term operation of the thruster source in positive polarity can lead to the formation of an electrochemical double layer that throttles the flow of liquid to the emitter tip. It was found that alternation of the polarity at 1 Hz was sufficient to eliminate such processes.[7] The time scale for the double layer build up to occur has been measured on the order of hours,[10] however, and we therefore expect no significant problems during the relatively short measurement time required to conduct the present experiments in positive DC mode.

The electrospray beam is sampled in the near field by moving one of several possible targets in place. A Faraday cup and a quartz crystal microbalance (QCM; XTM/2, Inficon), both with 6 mm entrance apertures, and a cylindrical lens element for beam transmission are mounted orthogonal to the beam axis on a translation stage, and are interchangeable. The Faraday cup and QCM characterize the electrospray plume by detecting current and mass flow as a function of thruster angle. The ratio of the mass flow to the current allows for an estimation of the average mass per emitted charge, m/q. The third near field target, the cylindrical lens element, allows the beam to pass through a 3 mm diameter aperture, with a solid angle of acceptance of ~ 6 degrees. It is then focused and injected into a quadrupole mass spectrometer for mass analysis. Upon exiting the quadrupole the beam passes through a set of three retarding potential grids and is then detected by an off axis electron multiplier detector. The angular distribution of the emitted spray is recorded by measuring the mass spectrum as a function of thruster angle. Alternatively, the energy distribution for a selected ion peak at a specific thruster angle can be measured by recording the depletion of the ion beam at the detector as a function of the voltage applied to the retarding potential analyzer. Both positive and negative ions are studied in this experiment.

III. Results

A. Nearfield Measurements

Table 1 lists typical experimental values of the electrosprayed plume measured using the near field Faraday cup and QCM targets, for high and low extractor voltages at both vertical and horizontal ribbon orientations, as well as positive and negative ribbon polarities. The measurements are made at the center of the thruster emission, along the z axis in Fig. 1. The ratio of the total emission current to the current measured on the Faraday cup gives an estimate of the spray divergence. A large average m/q value is observed for all emitter conditions, indicative of droplet formation, with no evidence of ion-only emission detected here.

Table 1. Typical electrospray parameters determined for [Emim][Im] wetted on a tungsten ribbon emitter

Ribbon Orientation	Vertical				Horizontal			
Polarity	+	—	+	—	+	—	+	—
V_{ext}	1080	1150	1350	1400	1100	1070	1300	1300
Total emission current (nA)	170	176	324	302	186	183	324	328
Faraday cup current (nA)	23.5	26.7	42.3	50.9	31.3	21.0	44.3	43.9
Mass flow (ng/s)	11.0	13.7	58.4	54	21.6	12.0	88.0	91.6
m/q (amu)	45,000	49,000	133,000	102,000	67,000	55,000	191,000	201,000

Figure 2 shows Faraday cup and QCM measurements as a function of thruster angle at positive emitter polarity, for low and high extraction voltages and vertical and horizontal ribbon orientations. Several important comparisons and contrasts may be made by careful examination of these near field measurements. First, at low extraction voltage

(~1100 V), measureable amounts of current extend to relatively high spray angles, ±30 degrees on either side of the thruster center. The mass flow measurements both show a much narrower spray angle, ± 10 degrees. The slight negative deposition readings detected at the edges of the mass flow distribution are attributed to ion sputtering processes. Figure 2 also shows near field measurements taken at higher V_{ext}, 1300 – 1350 V, for both ribbon orientations. Compared to the lower extraction voltages, the total amplitudes of both the Faraday cup and the QCM readings are somewhat higher. The angular distribution of the current is similar to that seen at lower extraction voltage, but the QCM reading is dramatically different. Measurable mass flow signal is detected at angles of up ± 25 degrees, nearly as wide as that of the current.

Another comparison that should be made is between the vertical and horizontal orientation of the ribbon. Generally, the spray angles detected from the thruster are very similar in the two different configurations. The one major difference

Figure 2. The angular dependence of ion current and mass flow measured with a Faraday cup and a QCM meter in the near field with a positive ribbon polarity. The black squares are the current measurements (left axis of each frame, nA), while the red triangles are the mass flow measurements (right axis of each frame, ng/sec).

observed here is that the center of the emission from the horizontal ribbon at low V_{ext} occurs about - 7.5 – 10 degrees off from the thruster center. The center of the spray intensity occurring off the thruster axis is not seen at high V_{ext}, meaning that misalignment of the source is not responsible for the shift in emission angle. This is a reproducible effect that, as seen below, is confirmed by the mass spectrometric measurements.

Additionally, although Fig. 2 shows only positive polarity measurements, comparison to negative polarity data shows that the emitter polarity has little effect on the near field spray parameters, which is confirmed by the results tabulated in Table 1. The data shown in Fig. 2 are representative examples of typical experimental results, and the angular dependence and overall appearance of the spray is similar for both positive and negative polarities, assuming similar extraction voltage and thruster orientation.

B. Mass Spectra

Figure 3 shows the anion mass spectra obtained as a function of thruster angle from a vertical orientation of the ribbon at an extraction voltage of 1150 V. The two dominate peaks in the mass spectra correspond to Im⁻ at 280
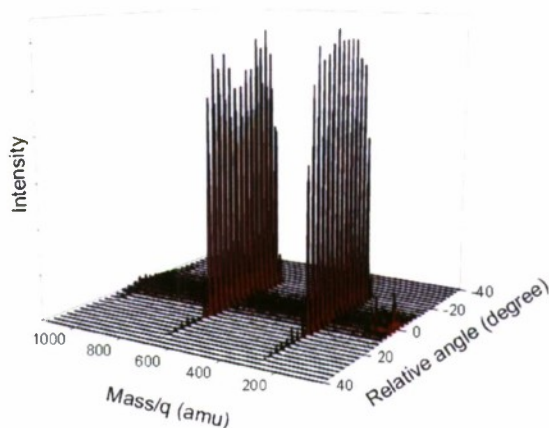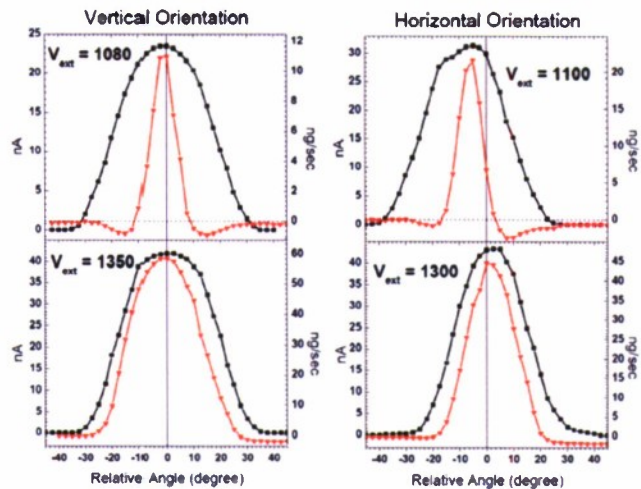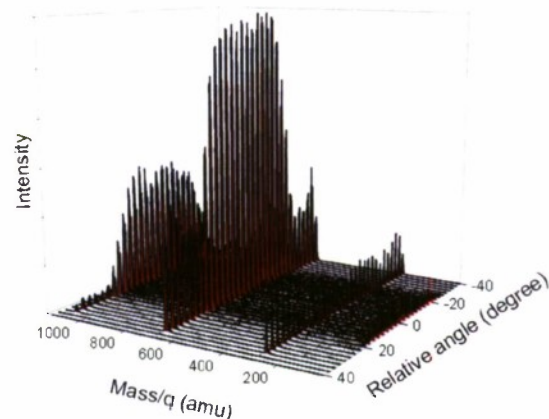

Figure 3. Anion mass spectra, recorded as a function of thruster angle, with the ribbon in the vertical orientation and V_{ext} = 1150 V.

Figure 4. Anion mass spectra, recorded as a function of thruster angle, with the ribbon in the vertical orientation and V_{ext} = 1400 V.

4
American Institute of Aeronautics and Astronautics

amu and Im⁻([Emim][Im]) at 671 amu, while Im⁻([Emim][Im])₂ at 1062 amu is observed with much less intensity. The ion signal shows an angular spread of about ± 20 degrees. The background detected throughout the mass spectrum at small angles is attributed to droplets with high m/q that are not rejected by the quadrupole mass analyzer. The angular distribution of this background is very similar to that seen for the mass flow in the near field measurements, which is consistent with the assignment of this signal to droplets. The average m/q for the particles along the center of the thruster axis under these emission conditions is ~49,000 amu. Figure 4 shows the anion mass spectra from a vertical ribbon obtained using a V_{ext} of 1400 V. In comparison to Fig. 3, the Im⁻ peak is much smaller relative to Im⁻([Emim][Im]), which now dominates the mass spectra, while the Im⁻([Emim][Im])₂ peak shows a significant enhancement in intensity. The spray angle is also much wider, with ion signal detected at ± 40 degrees from the thruster axis. Likewise the droplet background is seen at ± 20 degrees from the center, roughly twice the angular spread for 1150 V. The average m/q for the charged particles at the center of the emission axis is ~102,000 amu under these conditions.

Figure 5 shows the anion mass spectra as a function of angle with a V_{ext} of 1070 V produced from a ribbon mounted in the horizontal configuration. Similar to the lower voltage mass spectra in the vertical orientation (Fig. 3), the major mass peaks present are Im⁻ and Im⁻([Emim][Im]). The maximum angle of the spray is again roughly ± 20 from the center of the emission. However, as observed in the near field measurements for the horizontal ribbon at low extraction voltage, the spray is not centered about the thruster axis, but is approximately 10 degrees off to one side. This holds true for cation mass spectra studied at positive needle polarity as well (not shown). There is also a droplet background detected here, found at approximately ± 10 degrees from the center of the emission. The average m/q of the charges detected at the center of the emission, at -10 degrees, (not the thruster axis) is ~ 55,000 amu. Figure 6 shows the anion mass spectra as a function of angle for a horizontally mounted ribbon with an extraction voltage of 1300 V. The Im⁻(Emim][Im]) and Im⁻([Emim][Im])₂ cluster ions are again the most prominent mass peaks, whereas Im⁻ is present only with small intensity. The spray angle is ± 40 degrees about the center of the emission, which is now aligned with the center of the thruster axis. The droplet background is smaller here, but it can be seen faintly, and extends approximately ± 20 degrees from the emitter axis. The average m/q for the particles emitted in the center of the spray is estimated to be approximately 201,000 amu.
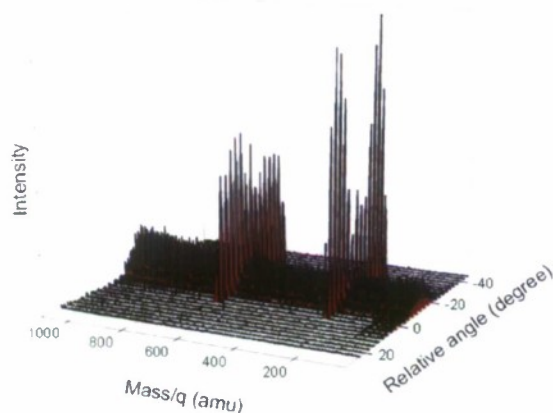

Figure 5. Anion mass spectra, recorded as a function of thruster angle, with the ribbon in the horizontal orientation and V_{ext} = 1070 V.
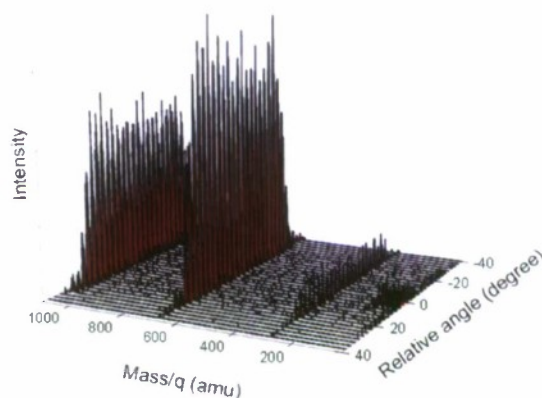
Figure 6. Anion mass spectra, recorded as a function of thruster angle, with the ribbon in the horizontal orientation and V_{ext} = 1300 V.

Cation mass spectra are also obtained as a function of thruster angle, at various extraction voltages, for both vertical and horizontal orientations of the ribbon emitter. The major cation peaks observed are Emim⁺ and Emim⁺([Emim][Im]) at low V_{ext} (~ 1100 V), while Emim⁺([Emim][Im]) and Emim⁺([Emim][Im])₂ are predominate at higher voltage. The measured spray angular distributions are likewise very similar for the two different electrospray polarities. Significantly, at low extraction voltage and in the horizontal ribbon configuration, the center of the cation mass spectra emission is located off the thruster axis, at the same relative angle as seen for the anions (~ -10 degrees). In both the anion and cation mass spectra, small features, attributed to fragment ions, are observed along the emission axis at low mass.

C. Ion Energy Analysis

Figures 7 and 8 display the retarding potential curves measured for the mass-selected $Emim^+([Emim][Im])$ ion using a horizontal ribbon configuration and extractor voltages of 1170 V and 1300 V respectively. The open circles represent the average of 3 or 5 scans and the solid line is the smoothed data. The insets of Figs. 7 and 8 show the corresponding energy distributions of the selected ions, obtained by plotting the derivative of the smoothed retarding potential curve. Both are measured at a thruster angle of 30 degrees. The ion energy distributions each show a single peak, but in Fig. 7, with the lower extractor voltage, the peak is centered at ~ 550 eV, close to the ribbon potential of 500 V. In Fig. 8, however, using higher extraction voltage, the peak is centered at ~ 400 eV, below the ribbon potential.
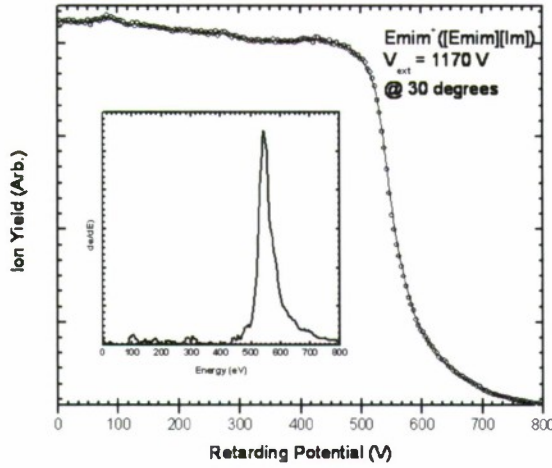

Figure 7. The retarding potential curve measured for $Emim^+([Emim||Im])$ at 30 degrees, with a horizontal ribbon orientation and V_{ext} = 1170 V. The inset is the corresponding energy distribution.

Figure 8. The retarding potential curve measured for $Emim^+([Emim||Im])$ at 30 degrees, with a horizontal ribbon orientation and V_{ext} = 1300 V. The inset is the corresponding energy distribution.

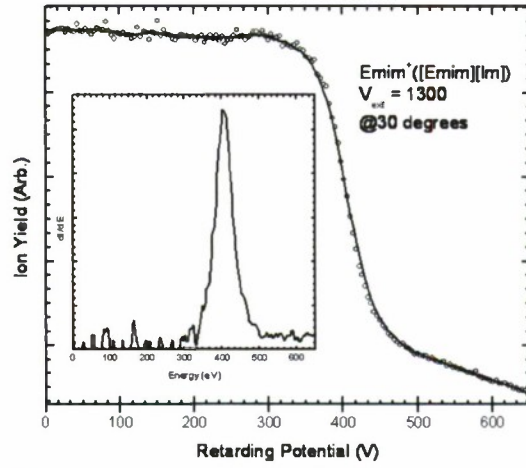The retarding potential curve obtained for mass selected $Im^-(Emim][Im])$ emitted on axis (0 degree angle) at 1350 V extraction with a vertical ribbon is shown in Fig. 9. Two step-like features are apparent here. The inset of Fig. 9 shows the corresponding energy distribution of the selected ions. Two main peaks are present in the energy distribution; a narrow, ~ 30 eV wide peak centered at ~ 530 eV, and a broader, ~70 eV wide peak centered at ~ 400

Figure 9. The retarding potential curve measured for $Im^-([Emim||Im])$ at 0 degrees, with a vertical ribbon orientation and V_{ext} = 1350 V. The inset is the corresponding energy distribution.

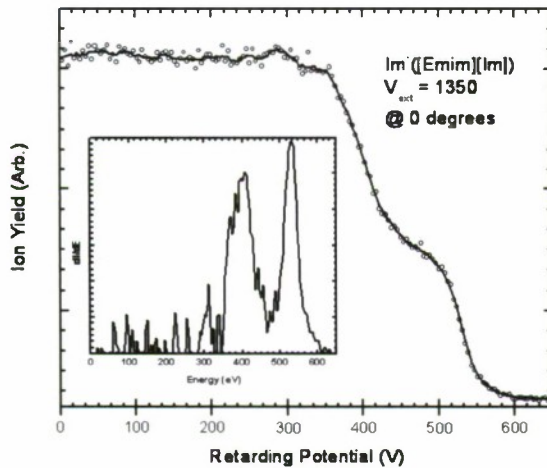**Figure 10. The retarding potential curve measured for $Im^-([Emim||Im])$ at 20 degrees, with a vertical ribbon orientation and V_{ext} = 1400 V. The inset is the corresponding energy distribution.**

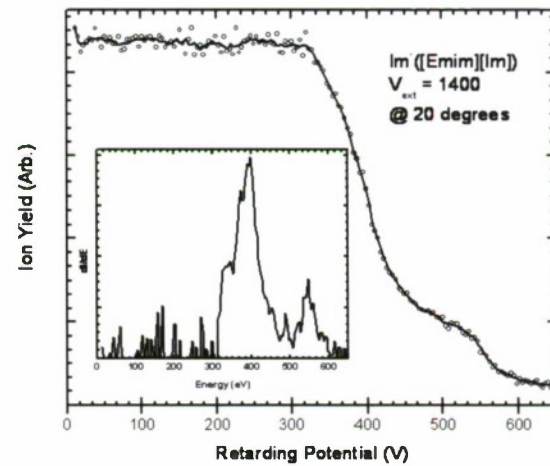American Institute of Aeronautics and Astronautics

eV. Figure 10 shows the energy distribution of the same ion, also from a vertical ribbon, with a V_{ext} of 1400 V at a thruster angle of 20 degrees. The inset shows the corresponding energy distribution, and again two peaks are apparent, a broader one centered at ~ 400 eV and a narrower one centered at ~ 540 eV. Compared to the ion energy distributions shown in Fig. 9, however, the peak at lower energy is much more intense than the higher energy one.

Retarding potentials and energy distributions were recorded for all ions (n=0,1,2) for positive and negative polarities at multiple angles, most not shown here for the sake of brevity. Generally, however, the ion energies directly correspond to the extraction voltage. At low extraction voltage, ions are observed at ~±500 eV, the emitter potential, while at high V_{ext}, ions are observed at energies significantly lower, ~±350 – 400 eV. At intermediate voltages, like that shown in Fig. 8, a combination of the ions at both energies is seen.

IV. Discussion

The combined near field measurements of current and mass flow, and the far field mass spectral data, all taken as a function of angle, show that two distinct modes of thruster operation can occur. The comparison of mass flow to current for low extractor voltage, in Fig. 2, shows that on axis the current is accompanied by large mass flow, while at large angles significant current is associated with negligible mass flow. This suggests that high m/q species (droplets) are emitted from the cone-jet near the thruster axis, while pure ion emission occurs at larger angles. These observations are both similar to previous experimental results obtained using needle emitters.[3, 9, 10] The use of a small V_{ext} favors a mixed ion-droplet emission regime centered along the emission axis, with ion emission detected at larger angles. With high V_{ext}, however, it seems that the thruster is operating in a different emission mode, one in which large m/q droplets are detected at even the large angles, and ion-only emission is no longer observed. The low extraction voltage result is similar to what was observed previously by Chiu et al for externally wetted tungsten needle emitters.[3, 9, 10] A sharpened needle has less surface area to accommodate propellant flow from the liquid reservoir to the emitter tip as compared to a sharpened ribbon. Thus the needle geometry effectively limits the maximum flow rate of the liquid to the end of the emitter. The ribbon, because of the additional surface area, can likely operate in either a low flow rate mode, approaching the limit achieved by a needle, or in a high flow rate mode. By using a low V_{ext} with the ribbon, the low flow rate of the needle is approached, accounting for the similarity of the experimental results. The emission characteristics of a ribbon operating at a high flow rate would likely be different, and the present work confirms this.

Both the previous needle and present ribbon experiments, however, are in contrast to the ion-only emission observed independently by the groups of Lozano[14] and Fernández de la Mora.[5, 11, 12] It was suggested at the time that the discrepancy between the previous experiments likely had to do with the radius of curvature of the emitter tips used, and that the ion-only emission mode was only possibly if a very sharp tip geometry, with a small radius of curvature, was utilized, limiting the flow rate of liquid to the tip.[9] For the ribbon case presented here, the surface area of the emitter leading up to the tip is certainly expected to be greater than that of the needles used in any of the previous experiments, producing the higher flow rates that necessarily accompany this geometry. Even using the extractor voltage to control the flow rate, it is apparently not possible to reduce it enough to reach the conditions required for ion-only emission from the ribbon. Previous experimental investigations, using capillary needles, a configuration in which the flow rate can be precisely controlled, showed that extremely high flow rates produce mainly droplets, with only low levels of ions present.[13] This model of electrospray emission at high liquid flow rates is similar to the results of the high extraction voltage experiments in the present work. As Fig. 2 illustrates, low V_{ext} produces droplets and ions on the thruster axis. The predominance of ions at larger angles is inferred from the negative mass deposition measured, which as mentioned above is attributed to sputtering of the QCM surface. As the voltage increases, however, the ribbon enters a different emission mode, where droplets are formed at even the largest angles of the spray. The dramatic increase in the mass flow (~ x 3-4) as the voltage increases also indicates that the thruster is operating in a different emission mode.

The mass spectral data also support this picture of distinct emission modes. The spectra taken at low V_{ext}, at vertical (Fig. 3) and horizontal (Fig. 5) orientation certainly have noticeable similarities. In both spectra, the Im⁻ and Im⁻([Emim][Im]) ions dominate, and the spray angle is relatively narrow, ~±20 degrees. The angular distribution of the droplet background is similar as well. The higher V_{ext} results, obtained at vertical (Fig. 4) and horizontal (Fig. 6) orientations, are also quite similar in terms of ion mass and angular distribution. The difference in the spray angle observed when using the lower V_{ext} versus the higher voltage is certainly notable. It has nearly doubled, from ±20 degrees at low V_{ext} to ~±40 degrees with high V_{ext}. The constant mass spectral background, attributed above to the presence of droplets, though visible to some degree in all the spectra, actually appears more prominent in the low extraction voltage measurements (Figs. 3 and 5). At first, this observation seems to conflict with the idea that the higher extraction voltages produce higher liquid flow rates, which then in turn emit more droplets. This discrepancy

can be explained, however, by the detection efficiency of the droplets as a function of size. As noted above, the average m/q of the particles emitted at the low extraction voltage limit is ~49,000 amu and ~55,000 amu, respectively, for Figs. 3 and 5. The average m/q for the high extraction voltage, shown in Figs. 4 and 6, is ~102,000 and ~201,000 amu, respectively. The detection efficiency of these particles depends on the *energy* per charge, however, not the m/q. Because smaller droplets are expected to have a higher energy per charge than larger droplets, they will be detected more efficiently. Thus the background observed in the mass spectra is more prominent when smaller droplets are produced. Previous needle emitter experiments detected even larger droplet backgrounds, and the average m/q measured in those experiments was on the order of ~20,000 amu,[9, 10] smaller than low V_{ext} case studied here, which provides additional evidence that smaller droplets are actually detected more efficiently in this experiment.

The shift in the mass distribution from Im⁻ (and Emim⁺ for the cations, not shown) at low V_{ext} to Im⁻ ([Emim][Im])₂ (and Emim⁺([Emim][Im])₂) at higher voltages is also consistent with larger droplets forming at higher extraction voltages. Previous computational work on these cluster ions has shown that Im⁻([Emim][Im])₂ (and Emim⁺([Emim][Im])₂) are both thermally unstable at room temperature.[10] Outside of some cooling mechanism, the Im⁻ and Emim⁺ ions should be the dominant ions observed in the spray, which is in fact what is seen for the low V_{ext} case. Evaporative cooling, where particles boil off either charged or neutral species until their internal energy is below a certain threshold for cluster stability, has been invoked previously to explain the observation of the larger ionic clusters.[10] Although this experiment does not reveal the precise cooling mechanism that occurs, the mass spectral data certainly indicates that the ion cooling process is more efficient under high flow rate conditions where larger droplets are emitted from the thruster, as this is when the larger ionic clusters are favored. The mass distribution can thus be one clue for determining in which emission mode the thruster is operating.

The distribution of energies measured for individual ion masses, shown in Figs. 7-10, lends even more evidence to the idea of multiple thruster emission modes. Figures 7 and 8 both show the energy distributions for the same mass selected ion, Emim⁺([Emim][Im]), at the same thruster angle, with the same ribbon orientation (horizontal). In the lower extraction voltage case, Fig. 7, the ion energy is centered at ~ 550 eV, approximately the ribbon potential. In fact, ion energies of ~ 500 eV are found for all ions at low V_{ext}, regardless of thruster angle. This is the energy expected for an ion that is formed in the neck region of the cone-jet where the maximal normal electric field occurs. The observation of these ions at large angles (~30 degrees) is consistent with this prediction. Figure 8, however, with a higher V_{ext}, shows the ion energy centered at 400 eV, ~100 V below the ribbon potential. Similar to the low V_{ext} case, where all observed ions are at the emitter potential, at high V_{ext} ions at all measured angles have energies below the ribbon potential. This has been previously shown to be the result of ion production at either the tip of the cone-jet, where the jet pinches off to form droplets, or from the dissociation of droplets.[10] The present experiment cannot definitely distinguish between these two ion formation processes, but both are only possible under conditions in which droplets are emitted. The measured energy distributions are then consistent with the near-field and mass spectroscopic measurements, which show that the high flow rates produced from high V_{ext} result in droplet emission at wide angles. The picture suggested is one of mixed ion-droplet emission at low flow rates, with droplets found on axis and ion emission at large angles. The energy of the ions at the low flow rates shows that they form at the neck of the cone-jet. At higher flow rates, however, droplets are observed at spray angles similar to the ion angular distribution, and the ion energies show they are formed either in the breakup region of the cone-jet tip or from the droplets.

The two peaks in the Im⁻([Emim][Im]) energy distribution, in Fig. 9, indicate that ions emitted using an intermediate V_{ext} of 1350 V likely come from two different sources. The peak centered at ~ 530 eV corresponds to ions formed at the neck of the cone-jet, while the peak at 400 eV, as mentioned above, comes from ions formed farther along the jet, either at the cone-jet tip or from droplets. The relative intensities of the peaks are roughly equal, signifying that at this extraction voltage, the thruster simultaneously emits equal amounts of ions from the two distinct sources, and the measured energies of the ions then reveal from which emission mode they are produced. Interestingly, under the same intermediate emission conditions, at the same thruster angle, the Im⁻ ion energy distribution (not shown) is peaked at ~ 530 eV, while that of Im⁻([Emim][Im])₂ is peaked at ~ 400 eV. As mentioned above, Im⁻ is favored under low flow rate conditions, which also favor the production of smaller droplets, whereas Im⁻([Emim][Im])₂ is more efficiently formed under the high flow rate condition that produces bigger droplets and more efficient cooling. The observation is consistent with the idea proposed above that two different emission modes are occurring simultaneously, and they produce different mass and ion energy distributions.

Figure 10 shows the energy distribution of the same ion at a V_{ext} of 1400 V, at a thruster angle of 20 degrees. Two peaks are again present in the energy distribution, but here the relative intensity of the peaks is dramatically different, with the peak at 400 eV much more intense. If this peak does indeed represent ions formed from droplets,

American Institute of Aeronautics and Astronautics

the increase in its intensity with the increase in V_{ext} is logical. The higher voltage causes the emission of more and larger droplets, as evidenced by the larger m/q, which in turn leads to a larger percentage of the detected ions forming from droplets. The shift in emission mode, seen between Fig. 9 and Fig. 10, is achieved with only a small increase in V_{ext} of 50 V. This is apparently a big enough change to increase the flow rate and thus shift the emission mode almost entirely toward that observed for high extraction voltage. It also suggests that the ion energies can be a useful metric for determining at what point the shift in emission occurs.

The presence of two dramatically different ion and droplet emission modes, which are observed simultaneously at intermediate V_{ext}, in addition to the shift of the center of emission off the thruster axis at low V_{ext} in the horizontal ribbon orientation, raises the possibility that two Taylor cones form at two physically different sites along the sharpened tip of the ribbon. Different flow rates to the different emission sites, possibly related to the local radius of curvature, could explain the observed changes in spray dynamics. The favored site at lower V_{ext} is likely slightly to the side of the tip center, creating the off axis emission observed in both the near and far field measurements (Figs. 2 and 5). The lower flow rate necessary to achieve emission from this site is sufficient to generate smaller droplets in a mixed ion-droplet emission mode, but all the ions observed have energies ~500 eV, the ribbon potential. The second Taylor cone site, likely close to the center of the thruster tip, requires higher flow rates to sustain stable emission, and favors droplet formation even at large thruster angle. At high V_{ext}, emission from this second, larger Taylor cone is observed. At intermediate voltages, however, it is possible to create emission from both sites simultaneously. The transition of the emission from one location on the ribbon to another is more readily apparent when the ribbon is mounted in the horizontal orientation. This is because the shift in emission occurs in the same plane (xz plane in Fig. 1) in which the source rotates with respect to the apparatus axis, and thus the center of the emission intensity is observed off the central thruster axis. In the vertical orientation, emission still occurs from two distinct regions of the tip, but in this case the shift along the ribbon tip occurs orthogonal to the emitter axis of rotation (along the yz plane in Fig. 1). The relative height of the spray with respect to the thruster axis changes, rather than the angle, making the change more difficult to quantify. If in fact multiple Taylor cones are responsible for the different emission modes seen here, then an increase in V_{ext} should lead to an increase in the total emission current, which is consistent with the present experimental observations.[15] The current measured as a function of angle by the Faraday cup could also ideally be used to resolve the contributions of each of the two Taylor cones to the total spray current, giving additional experimental evidence for this hypothesis. Unfortunately, the resolution achieved by the current experimental setup is not adequate to fully accomplish this goal.

Because each ribbon is electrochemically etched individually, the precise dimensions and tip structure of the particular ribbon used in these experiments are unique to it alone and may prove difficult to exactly duplicate. This is especially true of the off axis emission at low extraction voltages, and the formation of multiple Taylor cones at different locations around the emitter tip. However, the larger goal of using the amplitude of the extractor voltage as a method to control the flow rate of an IL propellant to the tip of an externally wetted ribbon emitter, and thus drive the thruster into either a low flow or a high flow method of operation and the associated mixed ion-droplet emission mode, is expected to be generally applicable regardless of the exact local structure of the emitter tip.

A final point of comparison appropriate here is that of the vertical versus horizontal ribbon orientation. Outside of the shift in the center of emission intensity described above, few changes in the electrospray dynamics are observed when changing the ribbon orientation. The current, mass flow, and mass spectrometric measurements all have approximately the same angular distribution in both the horizontal and vertical ribbon configurations. This perhaps surprising result suggests that physically, the shape and emission characteristics of the Taylor cone-jets formed do not change significantly with the inherently unequal ribbon tip dimensions at the two orientations, and implies that the geometry of the Taylor cone is limited by the size of the smallest dimension (i.e. the thickness) of the ribbon.

V. Conclusion

The angularly resolved current, mass flow, and mass spectrometric measurements for [Emim][Im] wetted on a tungsten ribbon are reported. Two different mixed ion-droplet emission modes are observed, depending on the extraction voltage applied to the emitter tip. The change in emission mode is attributed to the change in flow rate of the liquid to the tip associated with the different extraction voltages. A lower voltage (~1100 V) produces a mixed ion-droplet emission regime, similar to that seen before for needle emitters. With high V_{ext} (~1400 V), however, predominately droplets are emitted. The angular distribution of the mass flow changes dramatically between the two modes. At low V_{ext}, the mass flow is mainly centered on the thruster axis, with mainly ions (and no droplets) detected at large angles. With higher V_{ext}, however, the current and mass flow have similar angular distributions and droplets are emitted at all detectable angles. The mass spectral data likewise shows a shift in both angular

9

distribution and mass distribution between the two modes. At low V_{ext}, $Im^-/Emim^+$ and Im^- ([Emim][Im])/$Emim^+$([Emim][Im]) dominate the mass spectra for the anions and cations, respectively. At higher V_{ext}, the increase in the number and size of the droplets produced favors, possibly by more efficient evaporative cooling, larger ionic clusters which are otherwise unstable at room temperature. Energy analysis of mass selected ions confirms this picture. At lower V_{ext}, the measured ion energies are close to the emitter potential, as would be expected for ions produced directly from the neck of the cone-jet. The ion energies at higher extraction voltage, however, are lower than the ribbon potential, signifying that they are produced at the tip of the cone-jet, possibly by the dissociation of larger droplets, and not directly from the neck of the cone-jet. At intermediate V_{ext}, ions with energies corresponding to both processes are observed, indicating both emission modes occur simultaneously.

The two emission modes are likely the result of the formation of two distinct Taylor cones, with different liquid flow properties to each. This picture is also supported by the shift in the center of the emission off the thruster axis for low V_{ext} when the ribbon is in the horizontal orientation. The formation of two Taylor cones at two different locations along the emitter tip is thought to be the result of the specific geometry unique to the particular ribbon used in these experiments. The use of the extraction voltage to control the liquid flow rate, and thus drive the emission mode of the thruster, should be widely applicable to all ribbon emitters of the same basic form.

Acknowledgments

References

[1]Fernandez de la Mora, J. "The Effect of Charge Emission From Electrified Liquid Cones," *J. Fluid Mech.* Vol. 243, 1992, p. 564.

[2]Fenn, J. B., Mann, M., Meng, C. K., Wong, S. F., and Whitehouse, C. M. "Electrospray ionization for mass spectrometry of large biomolecules," *Science* Vol. 246, 1989, p. 64.

[3]Chiu, Y., and Dressler, R. A. "Ionic Liquids for Space Propulsion," *Ionic Liquids IV: Not Just Solvents Anymore.* American Chemical Society, Washington DC, 2007, p. 138.

[4]Ziemer, J., Gamero-Castano, M., Hruby, V., Spence, D., Demmons, N., McCormick, R., Roy, T., Gasdaska, C., Young, J., and Connolly, B. "Colloid micro-newton thruster development for the ST7-DRS and LISA mission," *41st AIAA/ASME/SAE/ASEE Joint Propulsion Conference and Exhibit,* 2005, pp. AIAA 2005-4265.

[5]Romero-Sanz, I., Bocanegra, R., Fernandez de la Mora, J., and Gamero-Castano, M. "Source of heavy molecular ions based on Taylor cones of ionic liquids operating in the pure ion evaporation regime," *Appl. Phys.* Vol. 94, 2003, p. 3599.

[6]Garoz, D., Bueno, C., Larriba, C., Castro, S., Romero-Sanz, I., Mora, J. F. d. l., Yoshida, Y., and Saito, G. "Taylor cones of ionic liquids from capillary tubes as sources of pure ions: The role of surface tension and electrical conductivity," *J. Appl. Phys.* Vol. 102, No. 6, 2007, p. 064913.

[7]Lozano, P., and Martinez-Sanchez, M. "Ionic Liquid Ion Sources: Suppression of Electrochemical Reactions Using Voltage Alternation," *J. Colloids Interface Sci.* Vol. 208, 2004, p. 149.

[8]Lozano, P., and Martínez-Sánchez, M. "Ionic liquid ion sources: characterization of externally wetted emitters," *J. Colloid Interface Sci.* Vol. 282, No. 2, 2005, pp. 415-421.

[9]Chiu, Y., Gaeta, G., Heine, T. R., and Dressler, R. A. "Analysis of the Electrospray Plume from the EMI-Im Propellant Externally Wetted on a Tungsten Needle," *42nd AIAA/ASME/ASEE Joint Propulsion Conference & Exhibit.* Scaremento, CA, 2006, pp. AIAA 2006-5010.

[10]Chiu, Y., Gaeta, G., Levandier, D., Dressler, R. A., and Boatz, J. A. "Vacuum Electrospray Ionization Study of the Ionic Liquid, [Emim][Im]," *Int. J. Mass Spectrom.* Vol. 265, 2007, pp. 146-158.

[11]Castro, S., Larriba, C., Mora, J. F. d. l., Lozano, P., Sumer, S., Yoshida, Y., and Saito, G. "Effect of liquid properties on electrosprays from externally wetted ionic liquid ion sources," *J. Appl. Phys.* Vol. 102, No. 9, 2007, p. 094310.

[12]Castro, S., and Fernandez de la Mora, J. "Effect of Tip Curvature on Ionic Emissions from Taylor Cones of Ionic Liquids from Externally Wetted Tungsten Tips," *J. Appl. Phys.* Vol. 105, 2009, pp. 034903-1.

[13]Gamero-Castano, M., Hruby, V., Spence, D., Demmons, N., McCormick, R., Gasdaska, C., and Falkos, P. "Micro Newton Colloid Thruster for ST7-DRS Mission," *39th AIAA/ASME/SAE/ASEE Joint Propulsion Conference and Exhibit.* Huntsville, Alabama, 2003, pp. AIAA 2003-4543.

[14]Lozano, P. "Energy Properties of an EMI-Im Ionic Liquid Ion Source," *J. Phys. D: Appl. Phys.* Vol. 39, 2006, p. 126.

[15]Lozano, P., Glass, B., and Martinez-Sanchez, M. "Performance Characteristics of a Linear Ionic Liquid Electrospray Thruster," *29th International Electric Propulsion Conference.* Princeton, New Jersey, 2005, pp. IEPC-2005-192.

[16]Legge Jr., R. S., Lozano, P., and Martinez-Sanchez, M. "Farbrication and Characterization of Porous Metal Emitters for Electrospray Thrusters," *30th International Electric Propulsion Conference.* Florence, Italy, 2007, pp. IEPC-2007-145.